Front. Phys. 13(1), 136201 (2018)
DOI 10.1007/s11467-017-0703-9

RESEARCH ARTICLE

PEG-PLGA electrospun nanofibrous membranes loaded with Au@Fe_2O_3 nanoparticles for drug delivery applications

Salvatore Spadaro[1], Marco Santoro[1], Francesco Barreca[1], Angela Scala[2], Simona Grimato[1], Fortunato Neri[1], Enza Fazio[1,†]

[1] *Dipartimento di Scienze Matematiche e Informatiche, Scienze Fisiche e Scienze della Terra, Università di Messina, Viale F. Stagno D'Alcontres 31, 98166 Messina, Italy*
[2] *Dipartimento di Scienze Chimiche, Biologiche, Farmaceutiche e Ambientali, Università di Messina, Viale F. Stagno D'Alcontres 31, 98166 Messina, Italy*
Corresponding author. E-mail: [†] *enfazio@unime.it*
Received March 2, 2017; accepted May 17, 2017

A PEGylated-PLGA random nanofibrous membrane loaded with gold and iron oxide nanoparticles and with silibinin was prepared by electrospinning deposition. The nanofibrous membrane can be remotely controlled and activated by a laser light or magnetic field to release biological agents on demand. The nanosystems were characterized using scanning electron microscopy, Fourier transform infrared spectroscopy, nuclear magnetic resonance spectroscopy, and thermogravimetric analyses. The drug loading efficiency and drug content percentages were determined by UV-vis optical absorption spectroscopy. The nanofibrous membrane irradiated by a relatively low-intensity laser or stimulated by a magnetic field showed sustained silibinin release for at least 60 h, without the burst effect. The proposed low-cost electrospinning procedure is capable of assembling, via a one-step procedure, a stimuli-responsive drug-loaded nanosystem with metallic nanoparticles to be externally activated for controlled drug delivery.

Keywords Au@Fe_2O_3 nanoparticles, PEG-PLGA copolymer, pulsed laser ablation, electrospinning, drug delivery

PACS numbers 62.23.St, 61.25.he

1 Introduction

Electrospinning is a simple and versatile top-down method for generating ultrathin fibers from a wide range of materials, including polymers, composites, and ceramics, by applying electric shear stress [1]. During electrospinning, the polymer solution, which is typically highly viscous, is forced through a spinneret by a syringe pump and then subjected to a strong electric field. The resultant liquid jet evaporates under a controlled temperature and humidity, and the remaining semi-solid polymer fiber is deposited onto a collector. The fluid emission speed from the needle varies in the 2-200 m/s range, depending on the physical properties of solution and processing conditions [2]. This method produces non-woven membranes with individual fiber diameters typically ranging from 50 to 500 nm. These fibers form a large, interconnected porous network with a high surface-to-volume ratio that is ideal for a wide range of biomedical applications, such as drug and gene delivery, wound healing, and tissue engineering [3]. Electrospun nanofiber-based drug delivery systems generally involve the use of polymers as matrices for the incorporation of therapeutic agents. In addition, the use of polymer blends can improve the tunability of the physicochemical and mechanical properties of the drug-loaded fibers, which can be conveniently employed for local and controlled administration of drugs, i.e., as transdermal delivery systems or as implants releasing bioactive molecules, including proteins and anticancer drugs [4, 5].

*Special Topic: Water and Water Systems (Eds. F. Mallamace, R. Car, and Limei Xu).

The formation of polymer nanofibers and, in turn, the fiber diameter, porosity, and orientation as well as the collected mats are strongly affected by electrospinning parameters, such as the applied voltage, pumping rate, collector characteristics, and solution composition. Moreover, electrospinning parameters influence the drug distribution in the fiber cross-section and the subsequent release efficiency [6]. Generally, drugs entrapped in polymeric nanoparticles (NPs) are slowly released by passive diffusion during spontaneous hydrolysis of the polymer matrix [7]. Otherwise, active and controllable drug release can be achieved by incorporating thermally activated Au or Ag NPs in the polymer matrix, followed by laser light irradiation [8, 9]. In fact, the addition of noble metal NPs confers thermoplastic properties to the polymers and this endows the nanocomposite with peculiar optical properties, improving their performance in releasing the drug upon light irradiation. The localized and intensive heating of metallic NPs results in the thermal expansion of the polymer; thus, the drug starts to diffuse out and be released in an active and controllable manner. In this way, the design of drug-loaded metal/polymer nanocomposites can be appropriately tuned for on-demand control of the dose, timing, and duration of the drug release.

In addition, the engineering of a polymeric nanofibrous membrane designed for the simultaneous encapsulation of therapeutic agents, thermally activatable metallic NPs, and non-toxic iron oxide magnetic nanoparticles, is a technological challenge that that would enable controlled drug release at a specific target site in response to two external stimuli (light source and magnetic field) and also enable magnetic guidance of the drug to a specific tissue [10].

The present study is focused on the preparation of PEGylated-PLGA random nanofibrous membranes loaded with Au and Fe_2O_3 NPs, and containing silibinin (SLB), a flavonolignan with promising anti-neoplastic effects. The morphology, composition and structure of the nanofibrous membrane were characterized by means of scanning electron microscopy (SEM) combined with an energy dispersive X-ray (EDX) probe; further, nuclear magnetic resonance spectroscopy (NMR), thermogravimetric analysis (TGA), and infrared transmission spectroscopy (FTIR) were also employed.

2 Experimental

The SLB-loaded PEG-PLGA_Au nanocomposite with a PEG-PLGA/SLB weight ratio of 10:1 was prepared by an emulsion-diffusion method, as previously reported [8]. 175 mg of the PEG-PLGA_Au-SLB nanocomposite was dissolved in 2 mL of DMF (solvent volume was $\approx$ 10% in wt of the total polymer content) under constant stirring at room temperature for 1 h. Next, to obtain a typically highly viscous polymer solution suitable for electrospinning, a DCM solution of PLGA was added, leading to a 35% w/v polymer solution of PEG-PLGA_Au-SLB/PLGA.

Fe_2O_3 nanoparticles were synthesized by pulsed laser ablation in a PVA aqueous solution, which was prepared as follows: 7.5 g of PVA was dissolved in 30 mL of distilled water. The dispersion was heated under magnetic agitation up to 90°C and refluxed for 2 h. After cooling to the room temperature, the dispersion was diluted in water to obtain a 7.5% w/v final solution. Some details are reported in Ref. [11]. Afterwards, 2 mL of Fe_2O_3 NP solution in PVA (Fe_2O_3-PVA) was added dropwise to a solution of PVA in DMF (0.75 g of PVA in 8 mL of DMF) and stirred for 30 min at room temperature, to obtain a viscous solution similar to that of the PEG-PLGA_Au-SLB/PLGA nanocomposite.

Finally, 5 mL of Fe_2O_3-PVA in DMF and 5 mL of the PEG-PLGA_Au-SLB/PLGA in DMF were electrospun simultaneously using multiple emitters/nozzles, leading to the final PEG-PLGA_Au-SLB/PLGA@Fe_2O_3-PVA nanofibrous membrane.

The electrospinning deposition setup consisted of a coaxial two-way stainless steel needle (with an inner core capillary opening diameter of 0.8 mm and a sheath capillary opening diameter of 1.8 mm) that was held horizontally by a holder while a grounded aluminum plate collector was placed vertically, as shown in Fig. 1.

The needle was connected through short path silicone rubber pipes to two syringe pumps, equipped with 10-mL syringes, that enabled fluxing of the NPs-loaded polymers at a very low rate (about 1 cc/h). In particular,

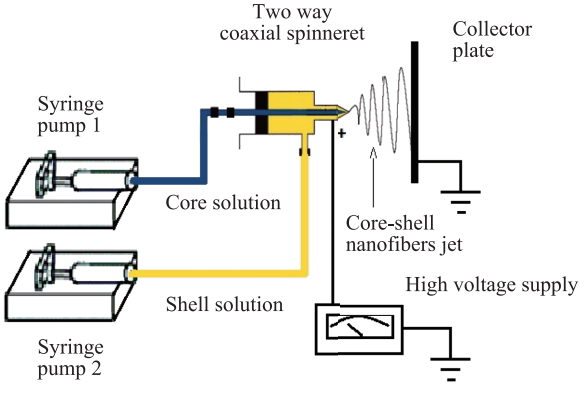

Fig. 1 Scheme of the electrospinning setup. In the figure, the core and shell solutions refer to Fe_2O_3-PVA and PEG-PLGA_Au-SLB/PLGA in DMF, flowing from the syringe pump 1 and syringe pump 2, respectively.

the Fe_2O_3-PVA and PEG-PLGA_Au-SLB/PLGA solutions were flushed through the inner core and sheath capillaries, respectively. The collector plate was covered with aluminum foil in order to collect nanofibers and positioned at a distance of 150 mm from the needle. A voltage of 30 kV DC was applied to the coaxial spinneret, and the solution jet from the needle was collected on the aluminum foil. Subsequently, the aluminum foil was removed from the collecting plate, and the nanofibrous membrane obtained was dried for at least 24 h. All experiments were performed at room temperature in controlled air-dry conditions.

^{1}H-NMR and ^{13}C-NMR spectra were recorded at room temperature using a Varian 500 MHz spectrometer. Chemical shifts (δ) were expressed in ppm using tetramethylsilane (TMS) as an internal reference.

The Fourier transform infrared (FTIR) spectra were recorded in the 4000–600 cm^{-1} range, using a Spectrum 100 Perkin–Elmer spectrometer in the attenuated total reflectance (ATR) configuration. Thermal degradation of the investigated copolymers was monitored by TGA using a Mettler Toledo TGA 851 apparatus (horizontal balance mechanism) in air. Each sample was placed in an open alumina crucible. The sample weight was 5 mg. The thermogravimetric weight loss curve was recorded as a function of the temperature. First, the samples were kept at 25°C under a 10 mL·min^{-1} air flow until balance stabilization, and they were then heated at the maximum programmed heating rate (nominally 1000°C min^{-1}). A constant heating rate of 10°C min^{-1} was employed. The balance sensitivity was 0.5 mg. The weight loss was calculated as the difference between the weights at room temperature and at 900°C.

SEM imaging were carried out using a Zeiss Merlin field emission electron microscope, equipped with a Gemini II column®. SEM measurements were performed with an acceleration voltage of 2 kV and at a working distance of 7 mm. The SEM apparatus was coupled with a Quanta EDX spectrometer to carry out energy dispersive X-ray (EDX) analysis. When the measurements were carried out in the transmission mode (STEM), the images were acquired at 30 kV and a working distance of 4 mm.

X-ray photoelectron spectroscopy (XPS) analysis was performed on a K-Alpha system from Thermo Scientific, equipped with a monochromatic Al Kα source (1486.6 eV), and operating with and analyzer in constant analyzer energy (CAE) mode with a pass energy of 50 eV. A spot size diameter of about 400 μm was adopted.

Raman spectra were acquired using the XploRA setup equipped with a 30 mW diode laser emitting the 638 nm wavelength, an Olympus BX40 microscope, and a Peltier CCD sensor. Spectra from several random positions on each specimen were collected on account of the possible spatial non-homogeneity of the samples.

To evaluate the drug loading, 1 mg of the PEG-PLGA_Au-SLB nanocomposite was dissolved in 4 mL of PBS, sonicated for 30 min, and centrifuged at 6000 rpm for 45 min to remove the free drug. The resulting solid was lyophilized and re-dispersed in PBS/DMSO (99:1) to determine spectrophotometrically the SLB loading in the nanocomposite, using the optical absorbance data at λ = 286 nm and the SLB molar extinction coefficient (ϵ_{286}) that was previously calculated. Thus, the drug content (DC) and the drug loading efficiency (DLE) were calculated with the following equations:

- DC (%)=(Drug weight in the NPs/Weight of the NPs)×100;
- DLE (%)=(Drug weight in NPs/Weight of drug used in formula)×100.

The release experiments were performed with the colloidal solutions and the corresponding membranes. Then, in one case, the release experiments were carried out by the dialysis method in 10 mM PBS at pH 7.4. 4 mg of PEG-PLGA_Au-SLB was dispersed in 4 mL of PBS, sonicated for 1 h, and placed in the dialysis bag (MWCO = 3.5–5 KDa Spectra/Por®). The sample was submerged in PBS (external bag: 15 mL) and kept at 37°C with constant stirring. At fixed intervals, 1 mL of the release medium was withdrawn, replaced with an equal volume of fresh PBS, and analyzed by UV-Vis spectroscopy.

Using the electrospun nanofibrous membrane, the in vitro release experiments were performed by immersing the electrospun nanofibrous membranes in 10 mM PBS at pH 7.4, with constant stirring, and kept at 37°C. Again, at fixed intervals, 1 mL of the release medium was withdrawn, replaced with an equal volume of a fresh one, and then analyzed by UV-Vis optical spectroscopy. The experiments were carried out in duplicates. For the laser light-triggered release experiments, a continuous He-Ne laser source (λ = 632 nm, energy density = 21 mW/cm^2) was used.

In order to assess the magnetic-responsive drug-release behavior, the investigated samples were subjected to alternating current magnetic fields (ACMF, 200 KHz). For the magnetic experiments, a 5 KW high-frequency generator was adopted. The used inductor was a water-cooled copper coil with 12 turns and a length of 90 mm and a diameter of 40 mm. When the alternating magnetic field was applied, the temperature was monitored using a pyrometer placed above the inductor. A reference measurement of the pure solvent (equivalent volume) was subtracted from the data of all the investigated samples.

3 Results and discussion

The PEG-PLGA copolymer was synthesized in anhydrous toluene at reflux in the presence of stannous 2-ethylhexanoate as the catalyst, as already reported in Ref. [8]. The success of the synthesis was confirmed by ^{1}H, ^{13}C NMR and FT-IR spectroscopy analysis (Fig. 2).

The ^{1}H NMR spectrum of PEG-PLGA in $CDCl_3$ [see Fig. 2(a)] is consistent with the structure of the copolymer, confirming its successful synthesis. In particular, multiplets at 5.2 ppm and 4.8 ppm are attributed to methine and methylene groups of the PLGA, respectively; the singlet at 3.64 ppm is assigned to the methylene group of PEG and overlapping doublets at 1.5 ppm are attributed to the methyl group of the PLGA units. In the ^{13}C NMR spectrum of the PEG-PLGA copolymer [see Fig. 2(b)], the six major resonances corresponding to the methyl, methylene, methine, and carbonyl groups of the PLGA and PEG segments were observed at 16.7 ppm (methyl of PLGA), 60.8 ppm (methylene of PLGA), 69.0 ppm (methine of PLGA), 70.5 ppm (methylene of PEG), 166.3 ppm (carbonyl of PLGA), and 169.3 ppm (carbonyl of PLGA). The FTIR spectrum of PEG-PLGA was compared with the standard spectra of free PEG and free PLGA to confirm the successful formation of the new ester linkage in the copolymer PEG-PLGA. In the IR spectrum of the copolymer PEG-PLGA, all the

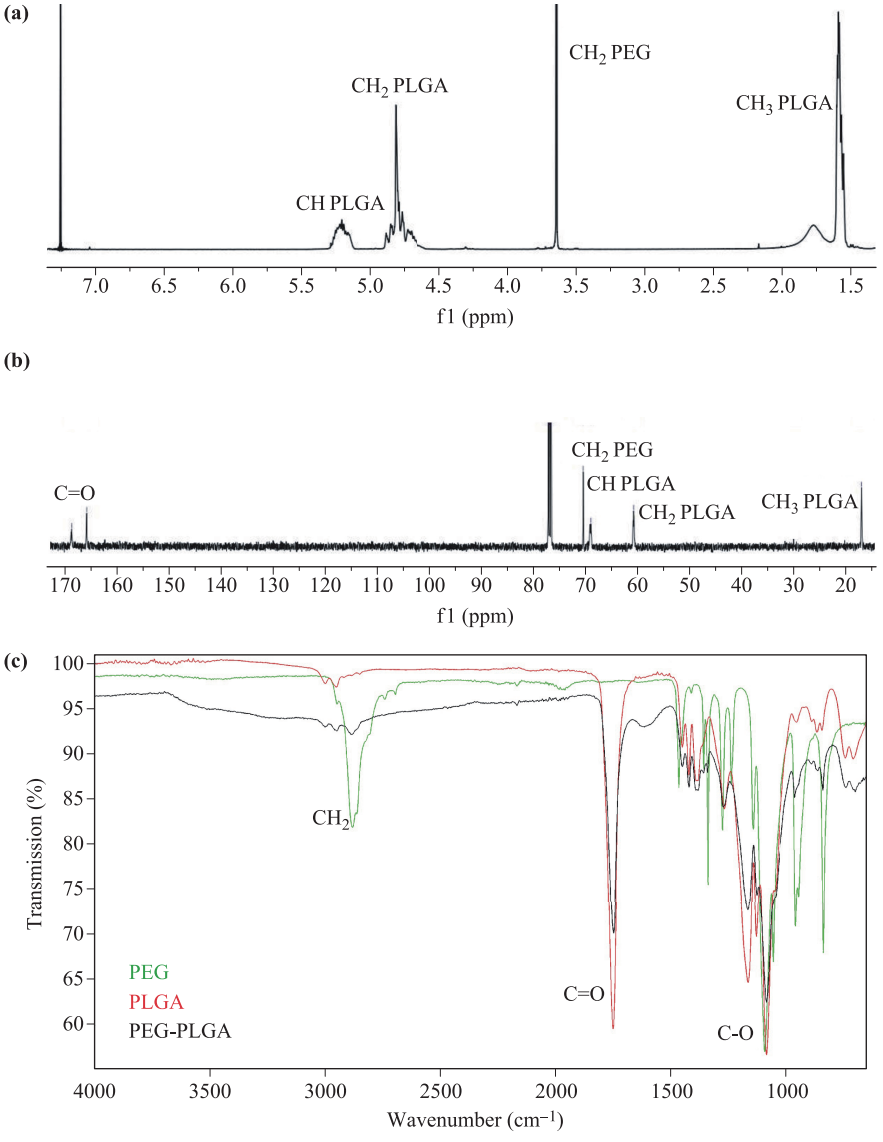

Fig. 2 ^{1}H NMR **(a)** and ^{13}C NMR **(b)** spectra of the copolymer PEG-PLGA in $CDCl_3$; **(c)** FTIR spectra of PEG, PLGA, and PEG-PLGA.

PLGA and PEG characteristic peaks are preserved and a shift of the carbonyl stretching frequency is observed from 1753 cm^{-1} for free PLGA to 1749 cm^{-1} for the PEG-PLGA copolymer [Fig. 2(c)].

^{1}H NMR measurements were further employed to obtain clear evidence of drug incorporation. Since PEG-PLGA are able to form core-shell NPs in an aqueous environment through a self-assembling process, we observe that PLGA and SLB peaks are absent in D_2O, while the characteristic peak of PEG is clearly evident [Fig. 3(a)], indicating that the water-soluble PEG backbone constitutes the outer shell, while the PLGA-based hydrophobic core is responsible for drug incorporation. Conversely, in DMSO-d_6, solvent in which the core-shell structure is disassembled, all the peaks of PEG, PLGA, and SLB are clearly visible [Fig. 3(b)].

The drug loading was determined spectrophotometrically on the lyophilized SLB-loaded PEG-PLGA dissolved in 99:1 PBS:DMSO. The amount of SLB was calculated using the intensity of the absorbance signal at the wavelength of 286 nm. On the basis of the optical absorbance data and known molar extinction coefficient value (ϵ_{286}) = 11320 $M^{-1}\cdot cm^{-1}$, SLB loading in the nanocomposite was 0.088 mg of drug per 1 mg of the drug carrier. We estimated that the drug loading efficiency is about 89% and the drug content is about 8.8%. On the other hand, the thermogravimetric analysis (TGA), under air flow, allowed to estimate that the percentage of Au and Fe_2O_3 into the polymers is about 1.5% and 0.9%, respectively. TGA analysis also shows that degradation starts later than in the electrospun scaffold [see Fig. 3(c)] The structure of the iron oxide particles was determined by carrying out Raman spectroscopy and XPS measurements on PEG-PLGA_Au-SLB/PLGA@Fe_2O_3-PVA. The Raman spectrum [Fig. 4(a)] is characterized by some contributions, centered at about 226.8, 292.5, 400, 486.5 and 600 cm^{-1}, ascribed to the Fe-O vibrational stretching mode, in hematite phase (α-Fe_2O_3) [12]. Fe 2p XPS lineshape [Fig. 4(b)] is characterized by two main contributions centered at 710.7 and 724.2 eV, respectively. The satellite peak at 719 eV is also evident, indicating that the hematite (α-Fe_2O_3) and maghemite (γ-Fe_2O_3) phases coexist on sample surfaces [13].

Finally, Au and Fe_2O_3 NP sizes and distributions in the polymeric composite were determined by using STEM images [Figs. 4(c), (d)]. The Au and Fe_2O_3 NP size ranges from 5 nm up to 50 nm.

SEM images of the sample after the electrospinning deposition are shown in Fig. 5.

Good quality nanofibers with smooth surface and without beads were obtained [see Fig. 5(a)]. The nanofibers, with an average diameter of about 200 nm, are spatially dispersed in random orientations, resulting in a three-dimensional porous net [see Figs. 5(b), (c)]. Therefore, the architecture of the electrospun membrane is composed of two parts, the macroscopic organization of the nanofibers and the secondary structure of the individual fiber arrangement [see Figs. 5(c), (d)].

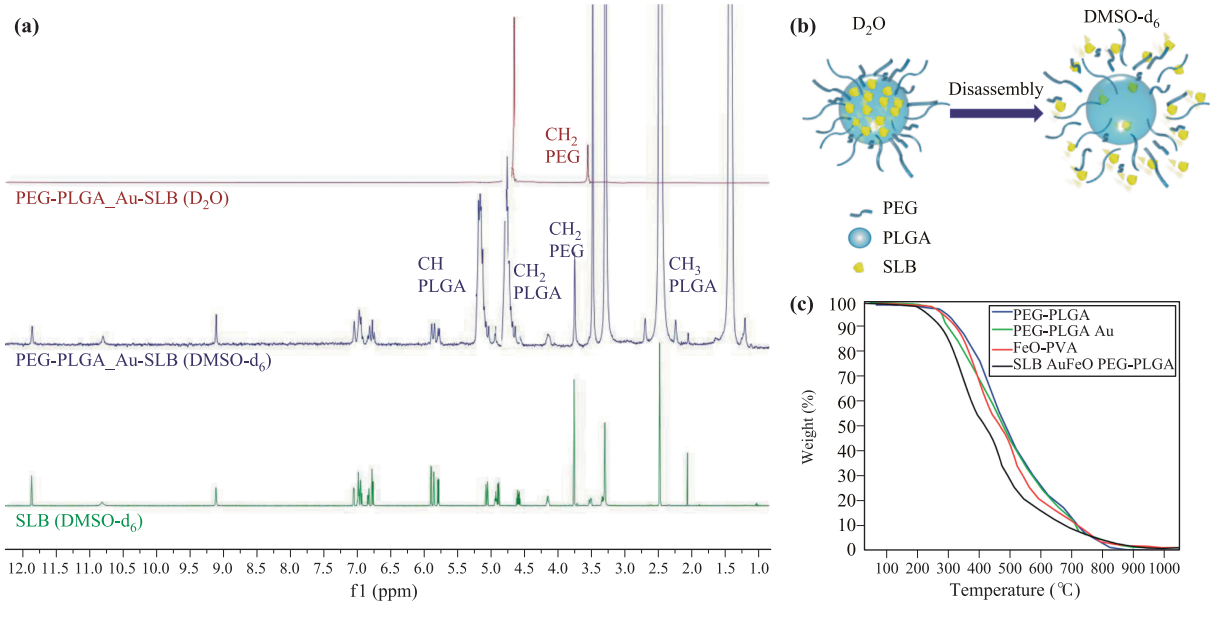

Fig. 3 ^{1}H-NMR spectra of SLB-loaded PEG-PLGA_Au in D_2O, SLB-loaded PEG-PLGA_Au in DMSO-d_6, and free SLB in DMSO-d_6, from top to down **(a)**. Schematic illustration of the assembly/disassembly of NPs in D_2O and DMSO-d_6, respectively **(b)**. TGA results for all investigated nanocomposites **(c)**.

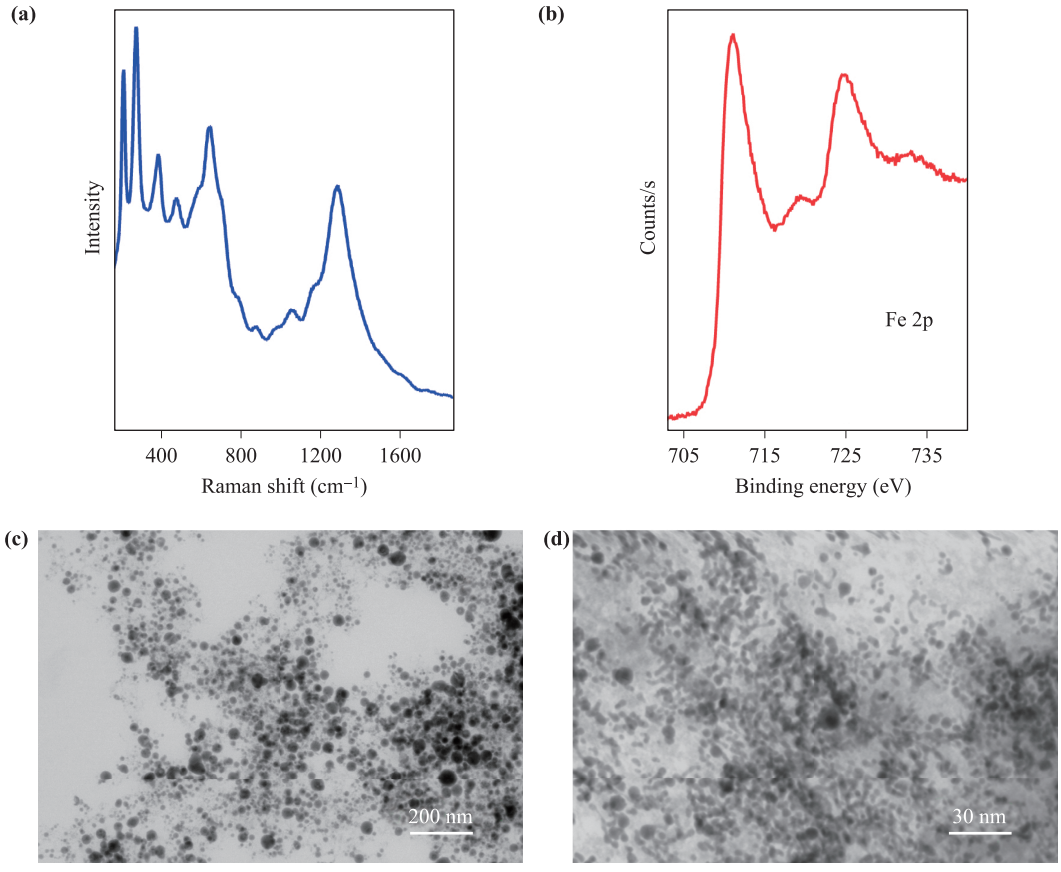

Fig. 4 Raman spectra **(a)**, XPS results **(b)**, and STEM images of Fe_2O_3 **(c)** and Au **(d)** NPs.

The random fiber deposition is explained by taking into account the fact that the elctrospinning deposition was carried out using a static collector plate configuration. SEM images show that the nanofiber polymeric surface is not decorated by Au and/or Fe_2O_3 nanoparticles [see Fig. 5(d)]. This evidence is supported by the results of XPS and EDX analyses. In fact, XPS probe does not reveal the presence of metallic NPs in the samples, indicating that they are embedded within the nanofibers. Otherwise, EDX probe (EDX detected pear-shaped dimension is about 0.7 μm while XPS probes only few nanometer in depth) collects the signals from Au and Fe atomic species. Thus, the composition of the system was determined by EDX analysis at different points of the sample. The estimated atomic percentage are: C (on average 80.5%), O (on average 19.2%), Au (on average 0.1%), and Fe (on average 0.2%).

Figure 6 shows the cumulative release of SLB observed for the irradiated electrospun sample and for the non-irradiated sample, as a function of time. For comparison, we also report the corresponding data for the colloidal samples before the electrospinning deposition. The drug is released more effectively upon light irradiation in an active and timely manner by the colloidal nanocomposite, as described in Refs. [8, 9], for analogous nanocomposites.

Regarding the membrane, a higher percentage of SLB (about 30% at about 40 h) is released upon irradiation with respect to the non-irradiated membrane. However, a slow response of the nanofibrous membrane toward the light stimulus is evident, probably due to the Au NPs distribution along the nanofibers.

Moreover, the investigated nanomaterials show interesting sustained responsive drug release induced by a magnetic field. The magnetization curves, acquired at room temperature, for all the investigated samples are shown in Fig. 7(a). No magnetization is observed in the PEG-PLGA_Au-SLB/PLGA since no Fe_2O_3 NPs are present. On the other hand, the magnetization of the PEG-PLGA_Au-SLB/PLGA@Fe_2O_3 in the membrane is lower than that of the PEG-PLGA_Au-SLB/PLGA@Fe_2O_3 in the corresponding solution. Moreover, no hysteresis loops (near-zero coercivity and remanence) is evident. In Fig. 7(b) the variation of the temperature as a function of time, in presence of the alternating magnetic field, is reported. Before ap-

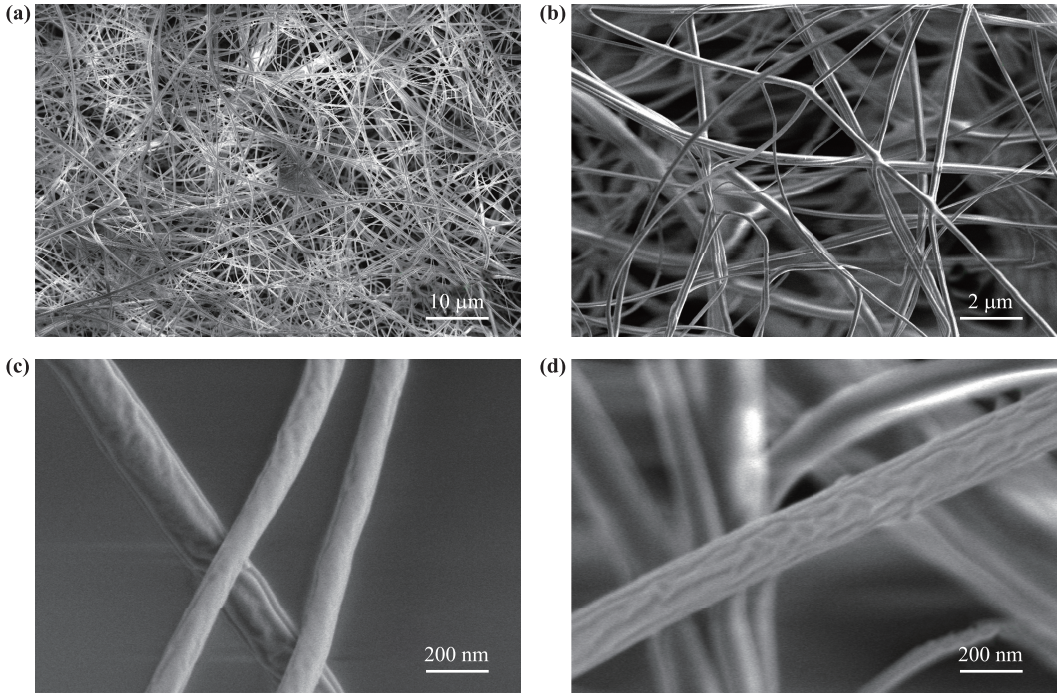

Fig. 5 SEM images of the nanofibrous membrane.

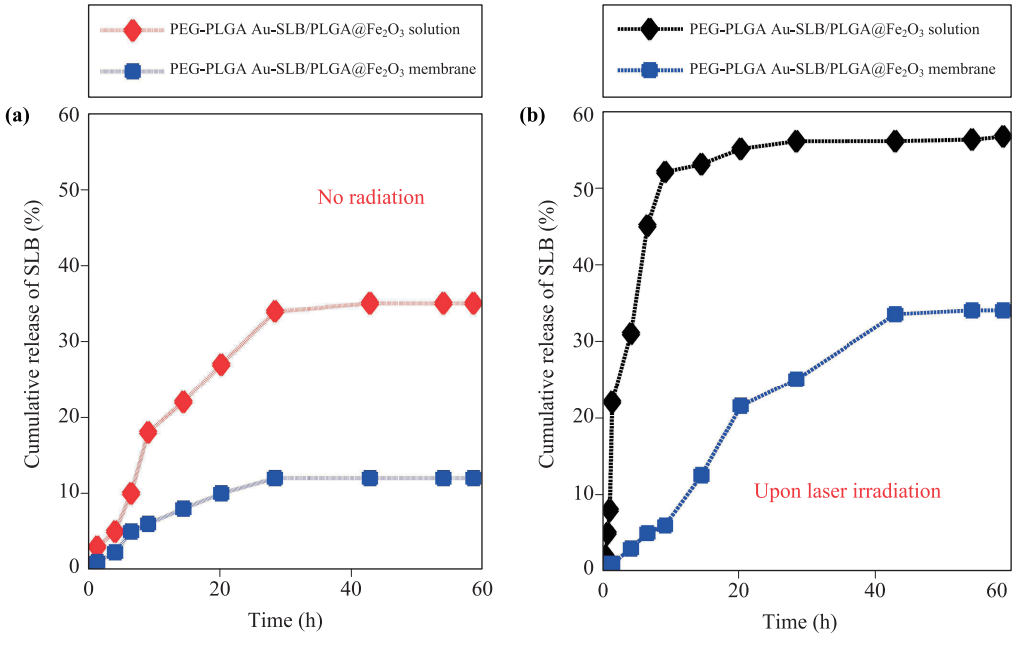

Fig. 6 Cumulative release of SLB as a function of time.

plying the magnetic field, the samples are maintained at 37°C. After 60 h, a temperature of 42°C and 44°C is reached for the solution and membrane, respectively. Under the external magnetic field, an initial fast release (within 20 h) followed by a relatively slow release during the time is observed [see Fig. 7(c)]. This behavior confirms that the magnetic field induces heating of the polymeric nanocomposites due to the delay in Neel relaxation of the magnetic moment [14], consequently triggers the release of the drug.

All these behaviors are explained by considering the relative contribution of the polymer degradation promoted by the Au@Fe_2O_3 mediated laser-magnetic irradiation heating effect.

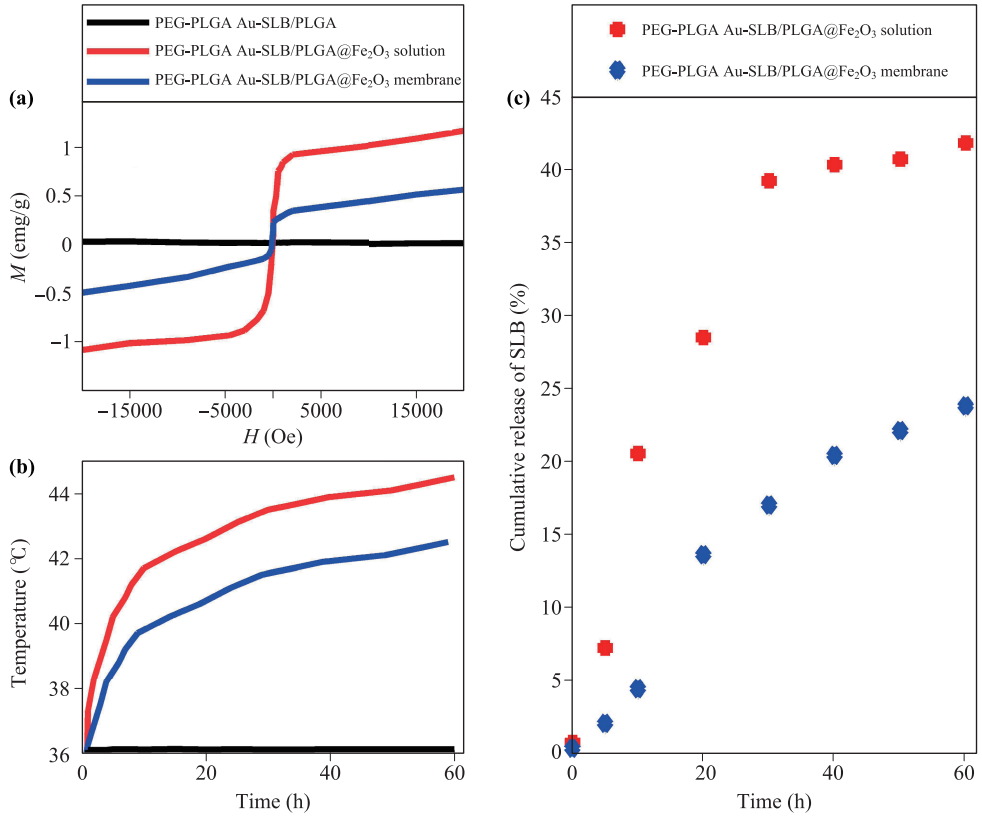

Fig. 7 Magnetization curves **(a)**; variation of temperature **(b)** and cumulative release of SLB **(c)** as a function of time.

Thus, the PEG-PLGA elctrospun nanofibrous membranes loaded with Au@Fe_2O_3 nanoparticles represent a multifunctional platform for laser-magnetic hyperthermia and local drug delivery. Nevertheless, the investigated nanocomposites can be optimized as a powerful delivery system for efficient light- and magnetic field-responsive drug release and chemo-thermal therapy.

4 Conclusion

A novel integrated plasmonic-magnetic nanofiber was fabricated and proposed as a remotely triggered nanoplatform for the entrapment and delivery of a poorly water-soluble drug. Passive drug diffusion, polymer swelling/degradation, matrix erosion, Au-mediated laser–irradiation-induced heating effect combined to magnetic one are responsible for the SLB release rate. However, by controlling the mode of encapsulation and the architecture of electrospun fibers, the drug release efficiency of the nanoplatform could be further optimized. Thus, the proposed nanovector could be advantageously activated by an external magnetic field, due to the presence of Fe_2O_3 NPs, and could also be applied for photothermal therapies that make use of visible optical radiation, due to the presence of Au NPs.

References

1. P. Raghavan, D. H. Lim, J. H. Ahn, C. Nah, D. C. Sherrington, H. S. Ryu, and H. J. Ahn, Electrospun polymer nanofibers: The booming cutting edge technology, *React. Funct. Polym.* 72(12), 915 (2012)
2. A. Krupa, A. Jaworek, A. T. Sobczyk, M. Lackowski, T. Czech, S. Ramakrishna, S. Sundarrajan, and D. Pliszka, Electrosprayed nanoparticles for nanofiber coating, ILASS 2008, 8-10.IX. 2008, Como Lake, Italy (Proc., Paper ID P-13)
3. K. C. Gupta, A. Haider, Y. Choi, and I. Kang, Nanofibrous scaffolds in biomedical applications, *Biomaterials Research* 18(1), 5 (2014)
4. S. Y. Chew, J. Wen, E. K. F. Yim, and K. W. Leong, Sustained release of proteins from electrospun biodegradable fibers, *Biomacromolecules* 6(4), 2017 (2005)
5. F. Zheng, S. Wang, M. Shen, M. Zhu, and X. Shi, Antitumor efficacy of doxorubicin-loaded electrospun nanohydroxyapatite–poly(lactic-co-glycolic acid) composite nanofibers, *Polym. Chem.* 4(4), 933 (2013)
6. Z. M. Huang, Y. Z. Zhang, M. Kotaki, and S. Ramakrishna, A review on polymer nanofibers by electrospinning and their applications in nanocomposites, *Compos. Sci. Technol.* 63(15), 2223 (2003)

7. T. T. Marquez-Lago, D. M. Allen, and J. Thewalt, A novel approach to modelling water transport and drug diffusion through the stratum corneum, *Theor. Biol. Med. Model.* 7(1), 33 (2010)
8. E. Fazio, A. Scala, S. Grimato, A. Ridolfo, G. Grassi, and F. Neri, Laser light triggered smart release of silibinin from a PEGylated–PLGA gold nanocomposite, *J. Mater. Chem. B Mater. Biol. Med.* 3(46), 9023 (2015)
9. F. Neri, A. Scala, S. Grimato, M. Santoro, S. Spadaro, F. Barreca, F. Cimino, A. Speciale, A. Saija, G. Grassi, and E. Fazio, Biocompatible silver nanoparticles embedded in a PEG–PLA polymeric matrix for stimulated laser light drug release, *J. Nanopart. Res.* 18(6), 153 (2016)
10. A. Hervault and N. T. K. Thanh, Magnetic nanoparticle-based therapeutic agents for thermo-chemotherapy treatment of cancer, *Nanoscale* 6(20), 11553 (2014)
11. E. Fazio, M. Santoro, G. Lentini, D. Franco, S. P. P. Guglielmino, and F. Neri, Iron oxide nanoparticles prepared by laser ablation: Synthesis, structural properties and antimicrobial activity, *Colloids Surf. A Physicochem. Eng. Asp.* 490, 98 (2016)
12. S. H. Shim and T. S. Duffy, Raman spectroscopy of Fe_2O_3 to 62 GPa, *Am. Mineral.* 87(2–3), 318 (2002)
13. V. Rebuttini, E. Fazio, S. Santangelo, F. Neri, G. Caputo, C. Martin, T. Brousse, F. Favier, and N. Pinna, Chemical modification of graphene oxide through diazonium chemistry and its influence on the structure-property relationships of graphene oxide-iron oxide nanocomposites, *Chemistry* 21(35), 1 (2015)
14. C. S. S. R. Kumar and F. Mohammad, Magnetic nanomaterials for hyperthermia-based therapy and controlled drug delivery, *Adv. Drug Deliv. Rev.* 63(9), 789 (2011)